Current Applied Physics 11 (2011) S185–S190

Contents lists available at ScienceDirect

Current Applied Physics

journal homepage: www.elsevier.com/locate/cap

Effects of thickness and annealing on the properties of Ti-doped ZnO films by radio frequency magnetron sputtering

Hung-Peng Chang, Fang-Hsing Wang*, Jen-Chi Chao, Chia-Cheng Huang, Han-Wen Liu

Department of Electrical Engineering and Graduate Institute of Optoelectronic Engineering, National Chung Hsing University, 250 Kuo-Kuang Rd., Taichung 402, Taiwan, ROC

ARTICLE INFO

Article history:
Received 7 September 2010
Received in revised form
29 November 2010
Accepted 29 November 2010
Available online 4 December 2010

Keywords:
Transparent conductive oxide (TCO)
Ti-doped ZnO (TZO)
RF magnetron sputtering
Annealing

ABSTRACT

Ti-doped ZnO (TZO) thin films were prepared by radio frequency magnetron sputtering with a target containing 1.5 wt% TiO_2 on glass substrates at 300 °C and then thermally annealed in a hydrogen ambient. The structural, electrical, and optical properties of TZO films were investigated with respect to the variation of film thickness and annealing condition. X-ray diffraction analysis exhibited that all TZO films had a (0 0 2) peak at 2θ ~34°, indicating that the films were hexagonal wurtzite structure and showed a good c-axis orientation perpendicular to the substrate. As film thickness increased from 30 to 950 nm, the crystallite size increased from 11.9 to 36.8 nm and the surface roughness increased from 0.57 to 1.78 nm. The film resistivity decreased from 3.94×10^{-2} to 1.06×10^{-3} Ω cm. To enhance the characteristics of TZO films for transparent conductive oxide applications, the films were subsequently annealed at temperatures ranging from 300 to 500 °C in hydrogen or argon ambient for various times. The results indicated that hydrogen annealing made film resistivity decrease more than argon annealing. The resistivity of the hydrogen-annealed film monotonically decreased with increasing annealing time up to 90 min. At the optimal annealing condition (400 °C, 60 min), the film resistivity decreased by 57% and the average optical transmittance in the visible wavelength range (400–700 nm) increased slightly as compared to the as-deposited films. The enhanced characteristics of the annealed TZO film are attributed to desorption of negative charged oxygen species and passivation of surface and defects at grain boundaries.

1. Introduction

Transparent conducting oxide (TCO) films such as indium tin oxide (ITO), tin oxide (SnO_2) and zinc oxide (ZnO) have been widely studied for applications such as solar cells, flat panel displays, and other optoelectronic devices [1–10]. Among these TCOs, ZnO is one of the most favorable materials because of its abundant, relatively low cost, good stability in hydrogen plasma process, and non-toxicity [5–10]. However, undoped ZnO thin films have unstable electrical properties because the sheet resistance of the films varies under either oxygen chemisorption or desorption. There is a considerable interest in understanding the electrical and transport properties of doped ZnO films. Many studies have found that the trivalent element-doped ZnO exhibits marked electrical conductivity [3–10]. Besides, Ti-doped ZnO (TZO) thin films are also possible alternative and have been reported previously [11–16]. Ti^{4+} has a radius of 0.68 Å, which is smaller than that of Zn^{2+}, 0.74 Å, and could be incorporated as an interstitial and acted as a scattering site. However, only a small amount of doped Ti^{4+} could induce more electrons and avoid acting scattering centers. Chung et al. [13] investigated the properties of Ti-doped ZnO films doped with different TiO_2 contents and reported that the lowest resistivity of TZO films was achieved as the Ti addition was 1.34%. Lin et al. [14] studied the effects of substrate temperature on the properties of TZO films by simultaneous RF and DC magnetron sputtering. Among these literatures, few studies report the influence of annealing on the characteristics of TZO thin films.

In this study, transparent conducting Ti-doped ZnO thin films were deposited on glass substrates by RF magnetron sputtering. The dependence of film thickness and annealing treatment on the structural, electrical, and optical properties of TZO thin films were investigated.

2. Experimental procedures

TZO thin films were deposited on glass substrates (Corning 1737) in a RF magnetron sputtering system with a ceramic target made of 98.5 wt% ZnO (99.999%) and 1.5 wt% TiO_2 (99.999%)

* Corresponding author. Tel.: +886 4 22851549x706; fax: +886 4 22851410.
E-mail address: fansen@dragon.nchu.edu.tw (F.-H. Wang).

1567-1739/$ – see front matter
doi:10.1016/j.cap.2010.11.110

powders. The substrates with an area of 33 × 33 mm^2 were cleaned with isopropyl alcohol (IPA) and deionized (DI) water, and then dried under blown nitrogen gas. The working distance was fixed at 10 cm. The base pressure was 5 × 10^{-6} Torr and the working pressure was maintained at 5 × 10^{-3} Torr. The deposition temperature was kept at 300 °C and the RF power was 100 W. The thickness of TZO thin films varied from 30 to 950 nm. The as-deposited TZO films with a thickness of 330 nm were subsequently annealed in a hydrogen or argon atmosphere at temperatures of 300–500 °C for different times using a horizontal furnace.

Film thickness was measured using a spectroscopic ellipsometer (Nano-view SE MF-100). Films crystallinity was analyzed using X-Ray diffraction (XRD) (PANalytical) with Cu-Kα radiation ($\lambda = 1.54056$ Å). Morphology of films was observed using field emission scanning electron microscopy (FE-SEM) (JEOL, JSM-6700) and atomic force microscopy (AFM) (Digital Instrument, NS4/D3100CL/Multimode). Electrical resistivity was determined by a four-point probe (Napson RT-70). Carrier concentration and Hall mobility were obtained from Hall-effect measurement by the Van der Pauw method (Ecopia, HMS-3000). Optical transmittance was measured by a UV/VIS/IR spectrophotometer (Jasco, V-570) in the 220–2500 nm wavelength range. All measurements were performed at room temperature.

3. Results and discussion

Fig. 1 shows the deposition rate of the TZO thin films for various thicknesses. When the film thickness ranged from 30 to 220 nm, the deposition rate decreased rapidly with increasing film thickness. As the film thickness increased beyond 220 nm, the deposition rate decreased slightly and finally saturated at about 8.3 nm/min. This phenomenon may be attributed to that the structure of the film tends to be porous and loose at the initial deposition stage; as the film thickness increases, the grains become densely packed [17].

Fig. 2 shows the XRD spectra of the TZO thin films deposited at 300 °C as a function of film thickness. All films exhibited a (0 0 2) peak at 2θ ~34°, indicating that the TZO films prepared by RF magnetron sputtering had a hexagonal wurtzite structure and showed a good c-axis orientation perpendicular to the substrate. The c-axis orientation in the TZO films can be explained by the "survival of the fastest" model proposed by Drift [18]. This result is similar with that of ZnO:Al and ZnO:Ga films [7,10,17]. Besides, there was no TiO_2 phase found from the XRD spectra, implying that titanium may replace zinc in the hexagonal lattice or segregate to the non-crystalline region in grain boundaries. When the film thickness increased from 30 to 950 nm, the positions of the (0 0 2) diffraction peaks are within 34.06° ± 0.03°. Moreover, the intensity

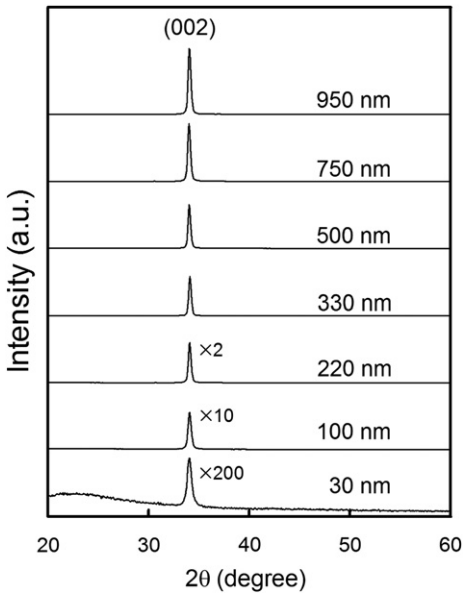

Fig. 2. XRD spectrum of the TZO thin films with various film thickness.

of the (0 0 2) peak increased with the increase of the film thickness. The XRD result indicates that the crystallinity of the TZO films improved as the films thickness increased.

Fig. 3 shows the dependence of the full width at half-maximum (FWHM) and grain size on thickness of the TZO thin films. The grain size can be estimated using Scherrer's formula [19],

$$D(\text{crystal size}) = (0.94\lambda)/(\beta\cos\theta) \quad (1)$$

where $\lambda = 1.54056$ Å and β is the FWHM. As the film thickness increased from 30 to 950 nm, the FWHM decreased from 0.81° to 0.26° and the grain size increased from 11.9 to 36.8 nm. As the film grows thicker, the larger grain is formed via the aggregation of small grains or grain boundary movement [20].

The dependence of the surface roughness on thickness of the TZO thin films was studied by AFM. Fig. 4 displays the AFM micrographs (1 μm × 1 μm) of the TZO films with various thicknesses. When the film thickness was very thin (30 nm), some hillocks occurred obviously, as Fig. 4(a) displayed, due to the film tending towards porous and loose. Ohring [21] has proposed that local mass flux divergences exist throughout the film due to varying grain size and distributions. When atoms come into a grain more than leave it, the pileup or growth of the mass can be expected. The

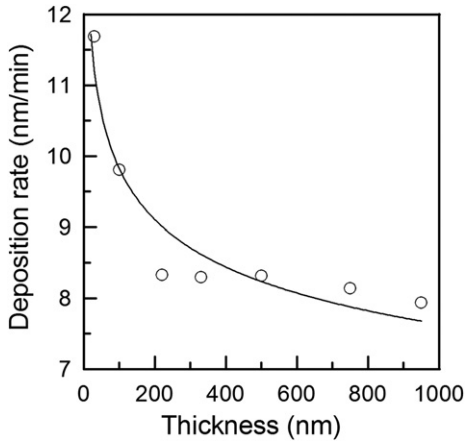

Fig. 1. Deposition rate of the TZO thin films as a function of film thickness.

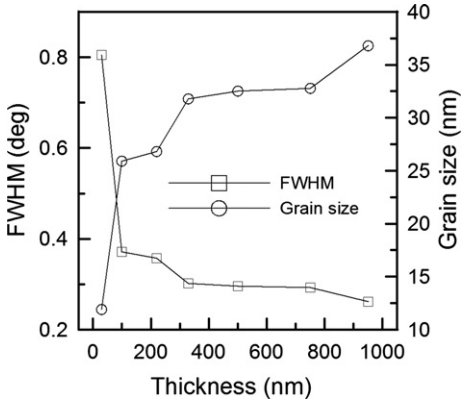

Fig. 3. Full width at half-maximum (FWHM) and grain size of the TZO thin films as a function of film thickness.

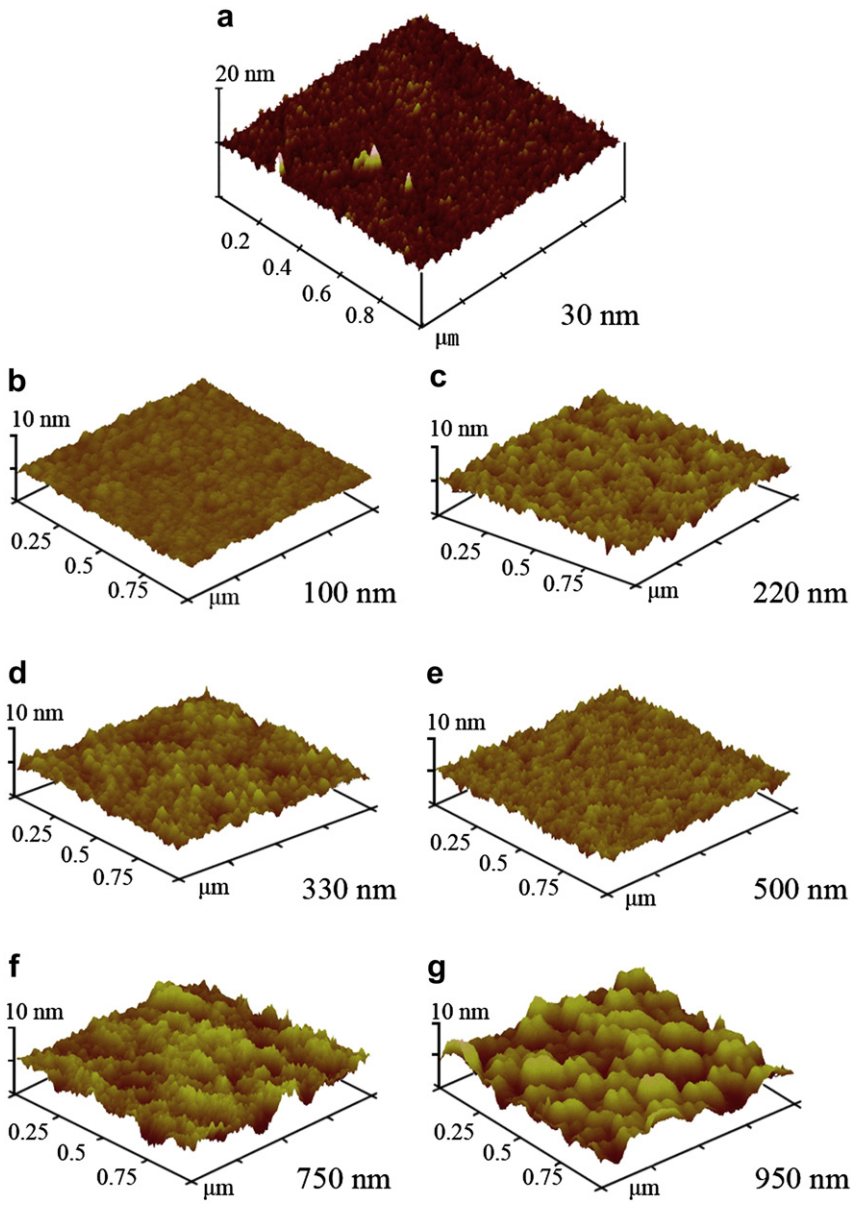

Fig. 4. AFM micrographs (1 μm × 1 μm) of the TZO thin films with different film thickness : (a) 30 nm (b) 100 nm (c) 220 nm (d) 330 nm (e) 500 nm (f) 750 nm (g) 950 nm.

measured root-mean-square (RMS) roughness of the TZO films increased from 0.50 to 1.78 nm when the films thickness increased from 30 to 950 nm. This result suggests that the thin film has smaller grain than the thick one. With increasing film thickness, the crystallinity is improved and the grain size becomes larger. This result is agreeable to the XRD observation. In addition, the surface of the TZO films prepared in this study was relatively smooth as compared to other TCO films such as Al-, Ga-, or In-doped ZnO thin films [4,7,22]. Yu et al. reported that the RMS roughnesses of the sputtered ZnO:Ga films at different powers were 4–13.5 nm [4]. Sim et al. reported that the RMS roughnesses of the undoped ZnO, AZO, GZO, and IZO thin films sputtered at 350 °C were 9.77, 2.37, 3.15, and 3.05 nm, respectively, as the thickness of all the films was fixed around 600 nm [22]. A smooth TCO surface is helpful to enhance its opto-electrical properties.

Fig. 5 shows the resistivity, Hall mobility, and carrier concentration of the TZO thin films as a function of thickness. The film resistivity decreased from 3.94×10^{-2} to 1.06×10^{-3} Ω cm when

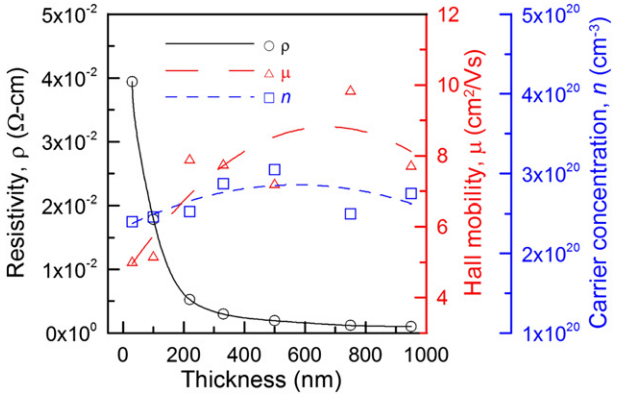

Fig. 5. Resistivity, Hall mobility, and carrier concentration of the TZO thin films as a function of film thickness.

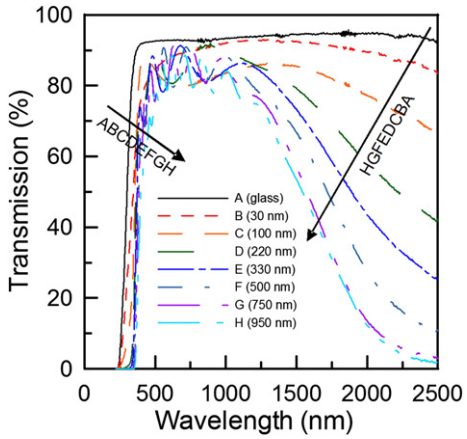

Fig. 6. Optical transmission spectra of the TZO thin films with various thicknesses in the wavelength region of 200–2500 nm.

the film thickness increased from 30 to 950 nm. The resistivity is a combined result from both the Hall mobility and the carrier concentration. For the decreased film resistivity, the Hall mobility and the carrier concentration both roughly increased with increasing film thickness due to improved crystallinity and intrinsic donors. The Hall mobility increased from 5.0 to 8–10 cm^2/Vsec and the carrier concentration increased from 2.40 $\times$ 10^{20} to nearly 2.80 $\times$ 10^{20} cm^{-3} for the film thickness above 330 nm.

Fig. 6 shows the optical transmission spectra of the TZO thin films with various thicknesses in the wavelength region of 200–2500 nm. The average optical transmission including the glass substrate in the visible wavelength region (400–700 nm) monotonically decreased from 85.4% to 76.7% with the increase of film thickness from 30 to 950 nm. In the near-infrared region, the transmittance decreased significantly as the film thickness increased. In the ultraviolet range, all the films showed a sharp absorption edge and it slightly shifted to the higher wavelength side with increasing film thickness. The corresponding optical bandgap (E_g) determined by applying the Tauc model and the Davis and Mott model [23] increased first from 3.448 to 3.518 eV when the film thickness increased from 30 to 330 nm. Then, E_g decreased gradually to 3.238 eV for further increasing the film thickness to 950 nm. The tendency of E_g roughly agrees with that of carrier concentration as shown in Fig. 5.

To improve the electrical properties of TZO films, the as-deposited TZO films were subsequently annealed in a hydrogen or argon atmosphere at different annealing temperatures and times. Table 1 lists the electrical and optical properties of the annealed TZO thin films with various annealing conditions. For the specimens annealed for different times, the film resistivity decreased with increasing annealing time to 90 min. Further extending the annealing time did not noticeably change the resistivity. It is believed that removal of depletion regions near grain boundary surfaces and formation of shallow donors contribute to the enhanced conductivity of the TZO films. These happenings are attributed to desorption of negative charged oxygen species and passivation of surface and defects at grain boundaries by hydrogen [10,24]. Oh et al. [10] proposed that the desorption of negatively charged oxygen species which act as trapping sites and form potential barriers resulted in the improvement of the carrier concentration and Hall mobility in the hydrogen-annealed ZnO:Al films. With increasing annealing time, the carrier concentration kept on increasing while the Hall mobility started to decrease after 60 min. Besides, XRD data (not shown here) exhibited inferior crystal quality for longer annealing time. It is thought that excess incorporated hydrogen atoms exist in the film and lead to deteriorated crystallinity and the decreased Hall mobility [16]. On the other hand, the average optical transmittance in the visible wavelength region (400–700 nm) for the as-deposited films was 83.4% and it slightly increased up to 84.1%, 84.5%, and 84.5% for the annealing time of 30, 60, and 90 min, respectively. The optical bandgap (E_g) estimated from the absorption edge increased slightly with increasing annealing time. The widened bandgap can be explained by Burstein–Moss effect [25], which specifies that the optical bandgap increases with increasing carrier concentration.

For the specimens annealed at different temperatures, the optimal annealing temperature was 400 °C and it made resistivity decrease by 57% (from 2.97 $\times$ 10^{-3} to 1.29 $\times$ 10^{-3} Ω cm). However, as the annealing temperature increased up to 500 °C, the resistivity increased significantly due to the film becoming loose and thin. This phenomenon could be observed by SEM images, as discussed later. On the other hand, the average visible transmittance increased from 83.4% to above 84.5% at the annealing temperatures of 300–400 °C. Moreover, a high visible transmittance of 90.9% was obtained when the sample was annealed at 500 °C due to the thin and loose TZO film after annealing. Previous research proposed by Yang et al. [26] indicated that porous surface was found on AZO thin films when annealing at 600 °C in N_2 ± 4% H_2 ambient. They explained that the N_2 + H_2 atmosphere has apparently etched the film. In the current study, the annealing gas of 100% H_2 and the Ti dopants may cause poor thermal stability of the film. The calculated optical bandgap of the films broadened from 3.510 to 3.530 and 3.548 eV as the annealing temperature increased to 300 and 400 °C, respectively. However, the degraded E_g (3.480 eV) for the 500 °C-annealed film was expectable as the film became loose and thin.

For the specimens annealed with different gas ambients, the films annealed in a hydrogen ambient possessed a lower resistivity than that annealed in an argon ambient. It is owing to passivation of surface and defects at grain boundaries contributing film conductivity during hydrogen annealing. The differences in average transmittance and optical bandgap between hydrogen and argon annealing were not apparent.

Fig. 7 displays the FE-SEM micrographs (with 45° tilt angle) of the TZO thin films annealed at various temperatures. As the annealing temperature increased to 300–400 °C, the films tended towards a compact structure. However, as the annealing temperature

Table 1
Electrical and optical properties of the annealed TZO thin films.

Sample	Annealing time (min)	Annealing temperature (°C)	Annealing gas ambient	Resistivity (Ω cm)	Hall mobility (cm^2/Vsec)	Carrier concentration (cm^{-3})	Average transmittance (%)	*Eg* (eV)
As-dep.	–	–	–	2.97 $\times$ 10^{-3}	7.84	2.47 $\times$ 10^{20}	83.4	3.518
T33H	30	300	H_2	2.23 $\times$ 10^{-3}	8.52	3.28 $\times$ 10^{20}	84.1	3.524
T63A	60	300	Ar	2.10 $\times$ 10^{-3}	–	–	84.6	3.528
T63H	60	300	H_2	1.97 $\times$ 10^{-3}	8.10	3.92 $\times$ 10^{20}	84.5	3.530
T93H	90	300	H_2	1.83 $\times$ 10^{-3}	6.48	5.26 $\times$ 10^{20}	84.5	3.533
T64H	60	400	H_2	1.29 $\times$ 10^{-3}	9.42	5.14 $\times$ 10^{20}	84.8	3.548
T65H	60	500	H_2	4.00 $\times$ 10^{-2}	–	–	90.9	3.480

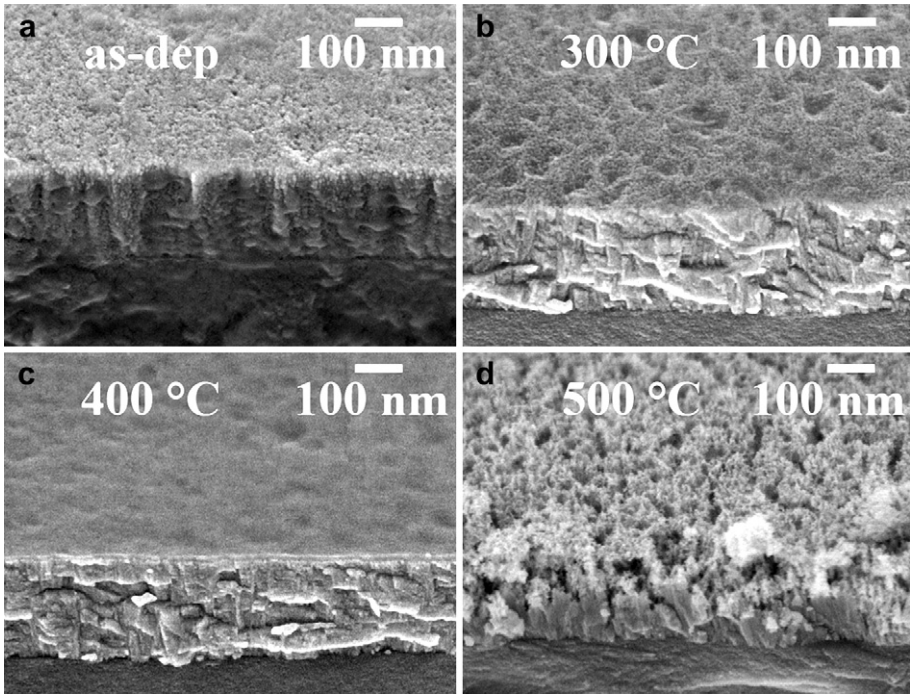

Fig. 7. FE-SEM micrographs (with 45° tilt angle) of the TZO thin films with various annealing temperature.

increased up to 500 °C, the film became thinner and looser because the film was etched under high temperature H_2 annealing. This result can explain why the film resistivity and the optical transmittance significantly increased at the high annealing temperature.

4. Conclusions

TZO thin films were deposited on glass substrates by RF magnetron sputtering. The structural, electrical, and optical properties of TZO films were strongly dependent on film thickness. The crystal structure of the TZO films was hexagonal wurtzite and the films were highly oriented along the c-axis perpendicular to the substrate. With increasing film thickness, the crystallinity was improved and the grain size became larger; the surface roughness of the film also increased slightly. The film resistivity decreased from 3.94×10^{-2} to 1.05×10^{-3} Ω cm and the average visible transmission decreased from 85.4% to 76.7% when the film thickness increased from 30 to 950 nm. Post-deposition annealing further improved the electrical and optical properties of TZO films due to the desorption of negative charged oxygen species during hydrogen annealing. The results indicated that the resistivity of the hydrogen-annealed film decreased with increasing annealing time to 90 min. For the films annealed at different temperatures, an improvement of 57% on resistivity was obtained at the optimal annealing temperature of 400 °C. Moreover, the hydrogen-annealed film had lower resistivity than the argon annealed one, revealing that hydrogen might passivate surface and defects at grain boundaries. In addition, annealing treatment also made the average optical transmittance in the visible wavelength region (400–700 nm) increase and the optical bandgap broaden.

Acknowledgements

Authors are thankful to the National Science Council of the Republic of China (Taiwan) for partly financial support under Contract No. NSC 95-2221-E-005-111.

References

[1] D.Y. Ku, I.H. Kim, I. Lee, K.S. Lee, T.S. Lee, J.H. Jeong, B. Cheong, Y.J. Baik, W.M. Kim, Structural and electrical properties of sputtered indium–zinc oxide thin films, Thin Solid Films 515 (2006) 1364–1369.
[2] D. Song, P. Widenborg, W. Chin, A.G. Aberle, Investigation of lateral parameter variations of Al-doped zinc oxide films prepared on glass substrates by rf magnetron sputtering, Sol. Energy Mater. Sol. Cells 73 (2002) 1–20.
[3] S.H. Lee, J.H. Jung, S.H. Kim, D.K. Lee, C.W. Jeon, Effect of incident angle of target molecules on electrical property of Al-doped ZnO thin films prepared by RF magnetron sputtering, Curr. Appl. Phys. 10 (2010) S286–S289.
[4] X. Yu, J. Ma, F. Ji, Y. Wang, X. Zhang, C. Cheng, H. Ma, Preparation and properties of ZnO: Ga films prepared by r.f. magnetron sputtering at low temperature, Appl. Surf. Sci. 239 (2005) 222–226.
[5] R. Das, T. Jana, S. Ray, Degradation studies of transparent conducting oxide: a substrate for microcrystalline silicon thin film solar cells, Sol. Energy Mater. Sol. Cells 86 (2005) 207–216.
[6] H.P. Chang, F.H. Wang, J.Y. Wu, C.Y. Kung, H.W. Liu, Enhanced conductivity of aluminum doped ZnO films by hydrogen plasma treatment, Thin Soild Films 518 (2010) 7445–7449.
[7] C. Li, M. Furuta, T. Matsuda, T. Hiramatsu, H. Furuta, T. Hirao, Effects of substrate on the structural, electrical and optical properties of Al-doped ZnO films prepared by radio frequency magnetron sputtering, Thin Solid Films 517 (2009) 3265–3268.
[8] W.M. Tsang, F.L. Wong, M.K. Fung, J.C. Chang, C.S. Lee, S.T. Lee, Transparent conducting aluminum-doped zinc oxide thin film prepared by sol–gel process followed by laser irradiation treatment, Thin Solid Films 517 (2008) 891–895.
[9] X.Y. Gao, Q.G. Lin, H.L. Feng, Y.F. Liu, J.X. Lu, Study on the structural, electrical, and optical properties of aluminum-doped zinc oxide films by direct current pulse reactive magnetron sputtering, Thin Solid Films 517 (2009) 4684–4688.
[10] B.Y. Oh, M.C. Jeong, D.S. Kim, W. Lee, J.M. Myoung, Post-annealing of Al-doped ZnO films in hydrogen atmosphere, J. Cryst. Growth 281 (2005) 475–480.
[11] R.G.S. Pala, W. Tang, M.M. Sushchikh, J.N. Park, A.J. Forman, G. Wu, A.K. Shwarsctrin, J. Zhang, E.W. McFarland, H. Metiu, CO oxidation by Ti- and Al-doped ZnO: oxygen activation by adsorption on the dopant, J. Catal. 266 (2009) 50–58.
[12] Y.R. Park, K.J. Kim, Optical and electrical properties of Ti-doped ZnO films: observation of semiconductor-metal transition, Solid State Commun. 123 (2002) 147–150.
[13] J.L. Chung, J.C. Chen, C.J. Tseng, The influence of titanium on the properties of zinc oxide films deposited by radio frequency magnetron sputtering, Appl. Surf. Sci. 254 (2008) 2615–2620.
[14] S.S. Lin, J.L. Huang, D.F. Lii, Effect of substrate temperature on the properties of Ti-doped ZnO films by simultaneous rf and dc magnetron sputtering, Mater. Chem. Phys. 90 (2005) 22–30.

[15] J.J. Lu, Y.M. Lu, S.I. Tsai, T.L. Hsiung, H.P. Wang, L.Y. Jang, Conductivity enhancement and semiconductor-metal transition in Ti-doped ZnO films, Opt. Mater. 29 (2007) 1548–1552.
[16] J.L. Chung, J.C. Chen, C.J. Tseng, Preparation of TiO_2-doped ZnO films by radio frequency magnetron sputtering in ambient hydrogen–argon gas, Appl. Surf. Sci. 255 (2008) 2494–2499.
[17] X. Yu, J. Ma, F. Ji, Y. Wang, C. Cheng, H. Ma, Thickness dependence of properties of ZnO: Ga films deposited by rf magnetron sputtering, Appl. Surf. Sci. 245 (2005) 310–315.
[18] A. Van der Drift, Evolutionary selection: a principle governing growth orientation in vapour-deposited layers, Philips Res. Rep. 22 (1967) 267–288.
[19] G. Sanon, R. Rup, A. Mansingh, Growth and characterization of tin oxide films prepared by chemical vapour deposition, Thin Solid Films 190 (1990) 287–301.
[20] J.C. Lodder, T. Wielinga, J. Worst, R.F.-sputtered Co-Cr layers for perpendicular magnetic recording I: structural properties, Thin Solid Films 101 (1983) 61–73.
[21] M. Ohring, The Materials Science of Thin Films. Academic Press, San Diego, CA, 1991, p. 379.
[22] K.U. Sim, S.W. Shin, A.V. Moholkar, J.H. Yun, J.H. Moon, J.H. Kim, Effects of dopant (Al, Ga, and In) on the characteristics of ZnO thin films prepared by RF magnetron sputtering system, Curr. Appl. Phys. 10 (2010) S463–S467.
[23] S. Mandal, R.K. Singha, A. Dhar, S.K. Ray, Optical and structural characteristics of ZnO thin films grown by rf magnetron sputtering, Mater. Res. Bull. 43 (2008) 244–250.
[24] G. Fang, D. Li, B.L. Yao, Fabrication and vacuum annealing of transparent conductive AZO thin films prepared by DC magnetron sputtering, Vacuum 68 (2003) 363–372.
[25] K.E. Lee, M. Wang, E.J. Kim, S.H. Hahn, Structural, electrical and optical properties of sol–gel AZO thin films, Curr. Appl. Phys. 9 (2009) 683–687.
[26] W. Yang, Z. Wu, Z. Liu, A. Pang, Y.L. Tu, Z.C. Feng, Room temperature deposition of Al-doped ZnO films on quartz substrates by radio-frequency magnetron sputtering and effects of thermal annealin, Thin Solid Films 519 (2010) 31–36.